

# Reactive Power Compensation and Voltage Support in Wind Farms Using PV-STATCOM (Case study at Adama-I Wind farm, Ethiopia)

HAGOS GEBREKIDAN BERHE  
 Electrical and Computer Engineering  
 Adama  
 ETHIOPIA  
 Email: [hagosg2005@gmail.com](mailto:hagosg2005@gmail.com)

**Abstract:** - The demand of electrical energy in general and the wind energy specifically is increasing worldwide. The challenges to this energy especially issues related with reactive power compensation and voltage support are increasing. Adama-I Wind Farm (WF) is one of these wind energy systems in Ethiopia. To compensate reactive power, the wind farm is using static capacitor banks and magnetically Coupled Reactors (MCR) type Static Var Compensators (SVC). However, the capacitor banks are not fast enough to alleviate the problem. To mitigate the problem of the existing wind farm, a new emerging technology photo voltaic-static synchronous compensator (PV-STATCOM) device is conducted at the main substation or point of common coupling (PCC) of the wind farm. The solar inverter is used to act as STATCOM, at the main substation or at Point of Common Coupling (PCC) for active power regulation and voltage/reactive power regulations during night-time and daytime. In this regard, 10 MVAR rated capacity of PV-STATCOM is needed to compensate the given reactive power depending on the capacitive reactive demand of the wind farm generators. For validation of the system, power world and MATLAB/PowerSim software are used for steady state analysis system and temporary over voltage analysis respectively.

*Key-Words:* - MATLAB/Simulink, PMSG, PV-STATCOM, Power World, PV-array, solar inverter

## 1. Introduction

### 1.1. Background

The development of wind energy in the entire world including in our country is increasing. In Ethiopia, most WFs are variable speed WECS (Adama-II and Ashegoda). The Adama-I WF is one of these variable speed WECS which is using a full converter controlled variable speed direct-drive (without gearbox) multi -pole permanent magnet synchronous generators. This variation in power output of the WTGs causes steady state voltage variation in the wind farm networks. Towards this, Adama-I wind farm has shunt capacitors and magnetically coupled reactor (MCR) type SVC to act as a reactive power compensators. However, capacitor devices are not fast enough to compensate the reactive power in the wind farm during sudden reactive current demand requirement in the WF network. Even, the MCR type SVC is an expensive device to use it only as reactive power compensator.

Due to single line to ground fault occurrences at the WF transmission network of Adama-I WTGs, voltage rise is occurred at the WTGs' side. The WTGs' are unable to withstand the voltage rise and disconnect them from the main grid repeatedly at a fault occurrence. And also the variation in voltage in the WF networks can reduce the capacity of the WTGs' connector transmission line.

In order to overcome the above problems, dynamic reactive power compensator, FACTS (STATCOM, SVC, etc) devices are widely used now days. STATCOM/SVC devices provide faster and smoother response to changes in voltage due to reactive power variation. However, these devices are expensive when used as only reactive power compensator/voltage regulators. Thus, the PV-STATCOM can solve the above problem with further benefits and that is the main reason for the selection of PV-STATCOM in this study.

This study concerns with steady state voltage variation and temporary voltage rise issues in grid connected PMSG based wind turbines.

**1.2. Grid Connected Wind Farm**

Generally, wind farms based on their grid connectivity are classified as grid connected and standalone wind farms. In this work, a grid connected Adama-I wind farm as shown in Fig.1.1, have been selected as a case study. Generally, this WF consists of wind, step-up unit transformers, WTG collecting and connector transmission line, wind turbine substation and the main grid transmission line. Where, wind turbine blades have connected to blade rotor, which, has fed to the generator shaft converts kinetic energy of the wind to mechanical energy, WTG convert the mechanical energy to an AC electric power from wind and then this power is filtered by generator side filter then rectified in to DC power by a rectifier. The DC power is boosted by using DC-DC boost converter, and then converted to AC power by the inverter. The output of inverter voltage is again filtered by grid side filter and stepped up to medium voltage level (33kV) with WTG unit transformer. Then the output of WTG unit transformer AC power /voltage is collected and transmitted to the wind turbine main substation. At the wind farm substation as shown in Fig.1.1 the substation transformer is used to step up the 33kV line voltage to 132kV line voltage of the main grid, then the main grid transmission line transmits this power to the national grid.

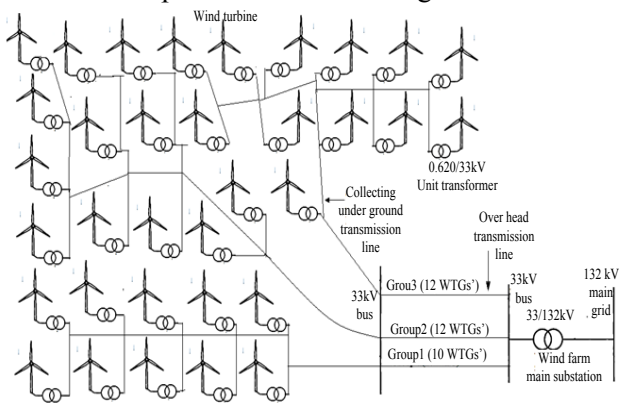


Fig.1.1. Grid connected Adama-I wind farm simple lay out diagram

**1.3. Wind Energy Conversion Systems**

As shown in Fig.1.3 the system consists of wind source, three blade turbine, direct derive permanent magnet synchronous generator (DD PMSG) diode bridge rectifier, DC-DC boost converter with associated controllers, DC link capacitor, inverter with controllers, AC filter, unit transformer and AC grid.

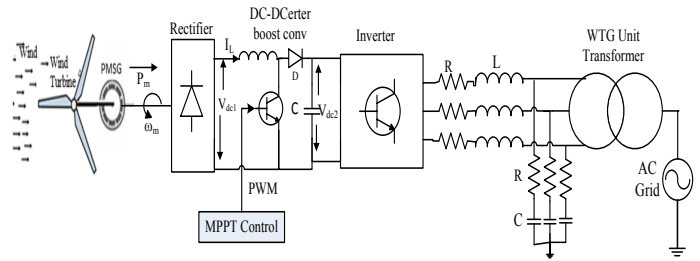


Fig.1.2.Single line electrical diagram of 1.5MW Adama-I WTG

From Fig.1.2 the selected place have a wind source with minimum wind speed of 3m/s and maximum of 12m/s. The three blades are connected to the turbine rotor which is coupled with shaft of the generator. The generator converts the mechanical power of the turbine blade to AC electric power. The AC power is converted DC power the bridge rectifier and boosted by DC-DC converter. The output of the boost converter is converted to AC power by the inverter. Then this power is filtered by RLC filter and stepped up by the unit transformer.

**1.4. Issues with Grid Integration of Wind Farms**

The major issues encountered by wind farm integration to the grid includes but not limited to this only are steady state voltage variation, increased temporary over voltage, voltage flicker and harmonic components and restrictions on operation of existing grid protection [2], [3]. In this work steady state, voltage variation and temporary over voltage is considered as a case study.

**1.4.1. Steady State Voltage Variation**

Connecting wind farms towards grid through transmission system may create power flow fluctuations depending on load condition. Traditionally, a transmission line is designed to carry designed amount of power from the source (grid) end towards the load end, is likely to face increased/decreased voltage at the PCC of WTG due to this power fluctuation [12].

From Fig.1.3, the voltage drop over the impedance  $Z_L$  is:

$$V_1 - V_2 = \sqrt{3} \times I(R_L + X_L) \tag{1.1}$$

Where;  $V_1$  is grid side voltage sources,  $V_2$  is the PCC voltage of the wind power,  $R_L$  is line resistance and  $X_L$  is line reactance.

At the point of connection of the wind farm, there is also a local load. The short circuit power,  $S_{PCC}$ , in the wind power PCC is:

$$S_{PCC} = \frac{V_2^2}{Z_L} \tag{1.2}$$

Changes in wind power generation will cause changes in the current through the impedance  $Z_L$ . This current changes cause changes in the voltage  $V_2$ .

The voltage  $V_2$  in the equation (1.2) is [12]:

$$v_2 = \left\{ -\frac{2\alpha_1 - v_1^2}{2} + \left[ \left( \frac{2\alpha_1 - v_1^2}{3} \right)^2 - (\alpha_1^2 + \alpha_2^2) \right]^{1/2} \right\}^{1/2} \quad (1.3)$$

Where;

$$\left\{ \begin{aligned} \alpha_1 &= -R(P_w - P_{LD}) - X(Q_w - Q_{LD}) \\ \alpha_2 &= -X(P_w - P_{LD}) + R(Q_w - Q_{LD}) \end{aligned} \right\}$$

Equation (1.3) shows that the reactive power production in the wind farm,  $Q_w$ , has an impact on the voltage  $V_2$ . This impact is dependent on the local load and on the feeding grid impedance. From this expression, we can identify that the interconnection voltage will increase or decrease depending on the power flow created by the difference between load and generation at the PCC ( $P_w - P_{LD}$ ), ( $Q_w - Q_{LD}$ ), the line reactance  $X_L$  and the line resistance  $R_L$ .

In this work, the impact of WFs at the PCC voltage variation is analyzed with ( $P_w - P_{LD}$ ) and ( $Q_w - Q_{LD}$ ).

The guidelines provided by IEEE standards (IEEE STD 1547-2003: IEEE standard for interconnecting wind farm resources with electric power systems) and CSA standards (CSA C22.3 No. 9-08: interconnection of wind resources and electricity supply systems) are widely implemented to specify the permissible steady-state voltage variation in medium voltage transmission line network. According to these standards, the steady state voltage limit of  $\pm 6\%$  of nominal value at the PCC terminal was permitted in Hydro China's technical interconnection requirements 2009. Appropriate reactive power compensation is required to maintain steady state voltage within permissible limits.

### 1.4.2. Temporary over Voltage

In medium voltage networks, unbalanced faults, SLGF in the network as shown in Fig.1.3 causes temporary over voltages on the healthy phases of the network line [1], [2]. Over voltages between one phase and ground or between two phases are classified based on the shape of the voltage, percentage increase from nominal value and duration of application. Temporary over voltages originating from switching or system faults (e.g. load rejection, unbalanced faults) or from nonlinearities (Ferro resonance effects, harmonics) are normally undamped or weakly damped [2].

In this study, SLGF have been considered as a base case study to observe the impact of temporary over voltages as shown in Fig.1.3.

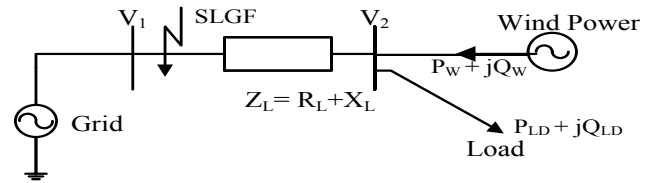


Fig.1.3. Single line to ground fault (SLGF) at the end of transmission line

The temporary rises in voltage are specified by IEEE standards and CSA standards. Based on these requirements, hydro china's networks has specified that the temporary over voltage anywhere in the distribution network under no circumstances shall not exceed 130%.

### 1.4.3. Mitigation Measures for Voltage Issues

**(1) Voltage support:** The installation of reactive power compensator devices may be required to operate in voltage regulation mode, that is, to adjust its reactive power production or consumption in order to control voltage on the local network [1].

If the network voltage decreases to a level below a pre defined range, an installation of capacitive reactive power compensator devices may be required to supply reactive power to the network to raise the voltage level. Conversely, if the network voltage increases to a level above a pre defined upper limit, then the installation inductive reactive power compensator devices would be required to consume reactive power to bring the voltage back within acceptable limits [1].

**(2) Reactive power compensation:** The effect of applying reactive power compensation to manage the voltage-rise effect and hence allow an increase in penetration of wind generation is achieved by absorbing reactive power at the PCC. In this case, active power generation would be curtailed only when the reactive power absorbed is insufficient for maintaining the voltage within permissible limits. To minimize losses and thus maintain high levels of efficiency, it is preferable that networks operate with voltage and current in phase that is, the power factor is unity.

In order to accomplish the reactive power control of the wind turbine either of the following methods can be used:

**Reactive power control:** The wind turbine is required to produce or absorb a constant specific amount of reactive power.

**Automatic voltage regulation:** The voltage in the wind turbine PCC is controlled. This implies that

WF is ordered to produce or absorb an amount of reactive power.

In this study, reactive power compensation to control of the WTGs' is achieved indirectly by regulating the PCC voltage.

Shunt capacitors and inductors provide fixed compensation. But, the variability of WECS requires a dynamic reactive power using FACTS (SVC, STATCOM etc...) devices.

**1.4.4. FACTS Controller based Mitigation Measures for Voltage Issues**

The FACTS devices are defined as the AC transmission systems incorporating power electronics based and other static controllers to enhance controllability and increase power transfer capability [4], [5], [6]. Due to their fast response and dynamic reactive power support capability, FACTS controllers were most suitable to mitigate voltage fluctuation.

**Static Synchronous Compensators (STATCOM):**

The STATCOM is the family of FACTS devices, which regulates voltage at its terminal by controlling the amount of reactive power injected into or absorbed from the power system [4].

Operation principle of STATCOM: A single-line STATCOM power circuit is shown in Fig.1.4 (a), where a VSC is connected to a utility bus through magnetic coupling (coupling transformer). In Fig.1.4 (b), a STATCOM is seen as an adjustable voltage source behind a reactance meaning that capacitor banks and shunt reactors are not needed for reactive-power generation and absorption, thereby giving a STATCOM a compact design, or small footprint, as well as low noise and low magnetic impact.

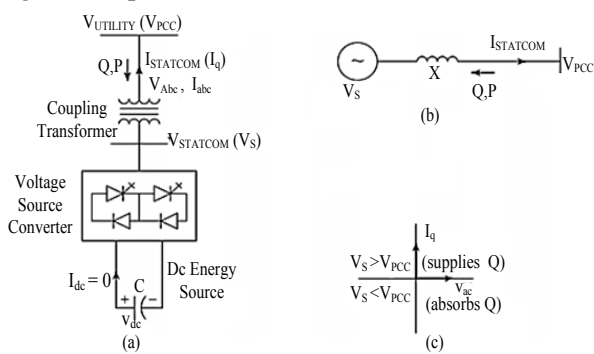


Fig.1.4. the STATCOM principle of operation diagram: (a) a power circuit, (b) an equivalent circuit, (c) a power exchange

Exchange of reactive power between the converter and the ac system (V<sub>pcc</sub>) is controlled by varying amplitude of 3-phase output voltage, V<sub>s</sub>, of the converter, as illustrated in Fig.1.4 (c).

From Fig.1.4 (a), the active and reactive power exchange between the utility (PCC) and STATCOM is given as:

$$P = \frac{(V_{PCC} \times V_s) \times \sin(\delta)}{X} \tag{1.4}$$

$$Q = \frac{V_{PCC} \times (V_{PCC} - V_s) \times \cos(\delta)}{X} \tag{1.5}$$

Where; V<sub>PCC</sub> is line to line voltage of the utility source, V<sub>s</sub> is line to line voltage output of STATCOM, X is reactance of interconnection transformer and filters and δ is phase angle of V<sub>PCC</sub> with respect to V<sub>s</sub>.

In steady state operation, the voltage V<sub>s</sub> generated by the VSC is in phase with V<sub>PCC</sub> (δ=0), so that only reactive power is flowing. If V<sub>s</sub> is lower than V<sub>PCC</sub>, Q is flowing from V<sub>PCC</sub> to V<sub>s</sub> (STATCOM is absorbing reactive power). On the reverse, if V<sub>s</sub> is higher than V<sub>PCC</sub>, Q is flowing from V<sub>s</sub> to V<sub>PCC</sub> (STATCOM is generating reactive power). Then the amount of reactive power is given by:

$$Q = \frac{V_{PCC} \times (V_{PCC} - v_s)}{X} \tag{1.6}$$

A capacitor connected on the DC side of the VSC acts as a DC voltage source. In steady state, the voltage V<sub>s</sub> has to be phase shifted slightly behind V<sub>PCC</sub> in order to compensate for transformer and VSC losses and to keep the capacitor charged. Any combination of real power generation or absorption with reactive generation or absorption is achievable if the STATCOM is equipped with an energy storage device of suitable capacity.

**2. Modelling and Control of Direct Drive Synchronous Generator based WTGs**

It has been noted that Adama-I WTGs are operating with low speed direct drive (gearless) multipole PMSG. The elimination of the gearbox improves the efficiency of the system and reduces initial costs and maintenance [1].

Adama-I WECS systems include the main control systems as shown in Fig.2.1.

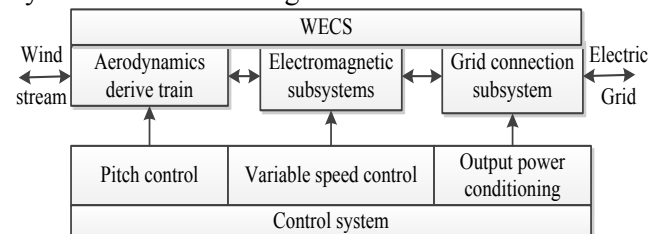


Fig.2.1. Main control subsystems of Adama-I WECS The first control subsystem affects the pitch angle following aerodynamic power limiting targets. The second implements the generator control, in order to obtain the variable-speed regime and the third

controls the transfer of the full (or a fraction) of electric power to the electric grid, with effects on WECS output power quality. The control structures result from defining one or more of the above goals stated in relation to a certain mathematical model of WECS as described in chapter four. The controller determines the desired global dynamic behavior of the system, such that ensuring power regulation, energy maximization in partial load, mechanical loads alleviation and reduction of active power fluctuations.

There are three aerodynamic methods to control the capture of power for large wind turbines which includes (1) Passive stall (2) Active stall, and (3) Pitch control. Since, Adama-I wind farm is used pitch angle control is studied.

**2.1.Wind turbine aerodynamics**

The rotor blades of the wind turbine capture only part of the available wind power:

$$P_m = \frac{1}{2} \rho \pi r^2 C_p(\lambda, \beta) v_w^3 \tag{1.7}$$

$$\left\{ \begin{array}{l} C_p(\lambda, \beta) = c_1 \left( \frac{c_2}{\lambda_i} - c_3 \beta - c_4 \right) \exp\left( \frac{-c_5}{\lambda_i} \right) \\ \text{Where; } \frac{1}{\lambda_i} = \frac{1}{\lambda_{opt} + 0.08\beta} - \frac{0.035}{\beta^3 + 1} \\ \lambda_{opt} = \frac{\omega_r \text{ (rad/s)} \times r \text{ (m)}}{v_w \text{ (m/s)}} \end{array} \right. \tag{1.8}$$

Where;  $\beta$  is the blade angle (pitch angle), and  $\lambda_{opt}$  is the optimal tip speed ratio of the wind turbine,  $\omega_r$  is the angular speed of the wind turbine generator. The values of the coefficients ( $c_1$ -to- $c_6$ ) depend on the type of the wind turbine. The relationships between  $C_p$  and  $\lambda$  are given in Fig.2.2.

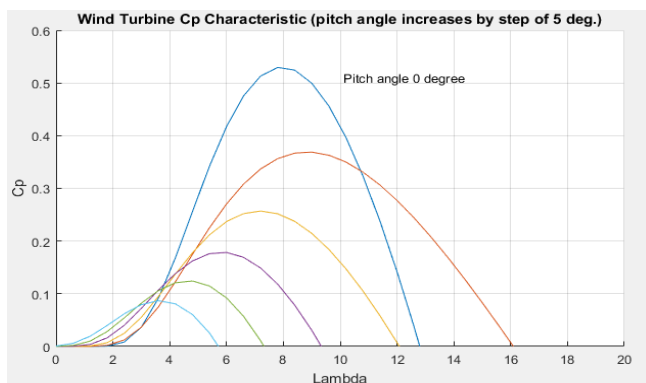


Fig.2.2. Characteristics function, CP vs.  $\lambda$ , at various pitch angle values for the studied WTG in MATLAB

**2.2. Wind turbine control system for MPPT**

In Adama-I wind farm, the DC-DC boost converter is controlled based on collective pitch

angle/rotor speed control method to extract maximum power as shown in Fig.2.3.

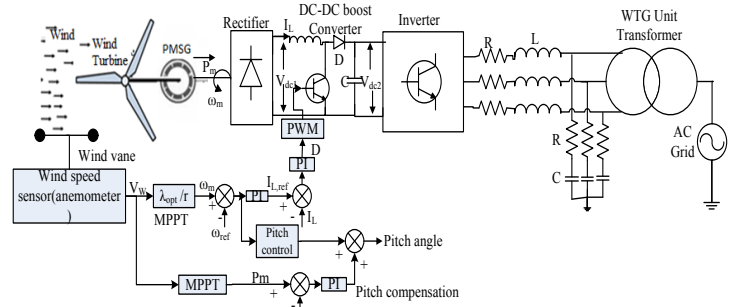


Fig.2.3. Collective pitch angle/rotor speed control diagram of Adama-I WTGs

**Tip Speed Ratio (TSP) Based MPPT:** In this method, the maximum power operation of the wind turbine is achieved by keeping the tip speed ratio to its optimal value  $\lambda_{opt}$  at pitch angle,  $\beta$  zero value. As shown in Fig.2.3, the measured wind speed  $V_w$  is used to produce the blade rotor (generator) mechanical speed  $\omega_m$ . By comparing the generator speed  $\omega_m$  with sated reference speed  $\omega_{ref}$  to generate the reference inductor current  $i_{Lref}$  of the boost converter and compared with the measured inductor current  $i_L$  of the DC boost converter, to generate the duty cycle  $D$ , which controls the ideal switch of the DC-DC boost converter to extract optimum power under fluctuating wind speeds. To reduce the error between reference inductor current  $i_{Lref}$  and measured inductor currents  $i_L$  is passed through PI controller. The mechanical speed of the WTG at MPPT extraction is given as:

$$\omega_m = \frac{\lambda_{opt}}{r} V_w = K V_w \tag{2.1}$$

**Pitch Angle Control Based MPPT:** The pitch angle controller in Fig.2.4 controls the mechanical power output,  $P_m$  of the WTG by controlling the mechanical speed,  $\omega_m$ . In lower wind speed conditions, the generated mechanical power,  $P_m$ , of the WTG is less than the actual reference mechanical power,  $P_{ref}$ . Here in the condition the pitch angle should be increased and compensated up to the maximum angle of attack to which the WT blade face to wind flow to gate more power. The measured mechanical power output,  $P_m$  of the WTG at MPPT is:

$$P_m = 0.5 \rho A C_{pmax} \left( \frac{r \times \omega_m}{\lambda_{opt}} \right)^3 \tag{2.2}$$

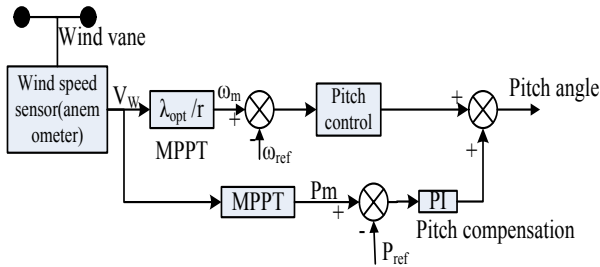


Fig.2.4. Block diagram of pitch angle control Adama-I wind turbine

**2.3. Grid-Side inverter Control based on Voltage Oriented with decoupled Control**

As the generator-side converter of the WTG controls the speed of the PMSG, the grid-side converter regulates the DC bus voltage while controlling the active power and reactive power injected into the grid. The active power and reactive power injected into grid is [7],

$$\begin{cases} P_g = 1.5(v_{dg}i_{dg} + v_{qg}i_{qg}) \\ Q_g = 1.5(v_{qg}i_{dg} - v_{dg}i_{qg}) \end{cases} \quad (2.3)$$

Where; the currents,  $i_{ag}$ ,  $i_{bg}$ , and  $i_{cg}$ , are the three phase AC grid currents.

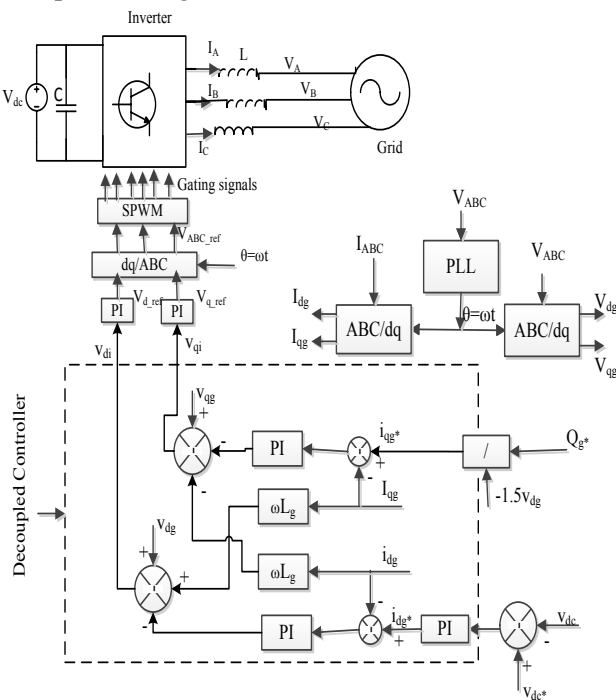


Fig.2.5. Voltage-oriented with a decoupled controller  
In Adama-I wind farm the grid side inverter of the WTG is controlled with VOC (Voltage Oriented Control) system. Even the system is simple in design and control system, it is not more stable in dynamic performance. To improve this stability voltage oriented with decoupled control system as shown in Fig. 2.5 has been used in this study.

Assuming that the controllers for the dq-axis currents in Fig.2.5 are of the PI type, the output of the decoupled controller is [7]:

$$\begin{cases} v_{di} = -(k_1 + k_2/s)(i_{dg}^* - i_{dg}) + \omega_g L_g i_{qg} + v_{dg} \\ v_{qi} = -(k_1 + k_2/s)(i_{qg}^* - i_{qg}) - \omega_g L_g i_{dg} + v_{qg} \end{cases} \quad (2.4)$$

Where;  $(k_1+k_2/s)$  is the transformation of the PI controller,  $\omega_g$  is the speed of the synchronous reference frame, which is also the angular frequency of the grid, and  $(\omega_g L_g i_{qg}$  and  $\omega_g L_g i_{dg})$  are the induced speed voltages due to the transformation of the three-phase inductance,  $L_g$  from the stationary reference frame to the synchronous frame. Equation (2.4) indicates that the decoupled control makes the design of the PI controllers more convenient, and the system more easily stabilized.

**2.4. Modeling of Solar Inverter as Conventional VSC based STATCOM: PV array inverter setup is analogous to the design of conventional STATCOM. As shown in Fig.2.6.**

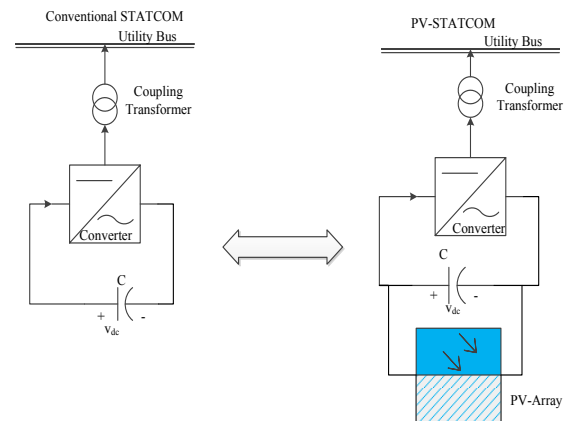


Fig.2.6. Conventional STATCOM versus PV - STATCOM comparison diagram

The main advantage that helps in utilization of PV inverter as STATCOM is having a DC output voltage from a PV array which is used as capacitor link in a conventional STATCOM as shown in Fig.2.6.

**2.4.1. Modes of operation of PV array based STATCOM**

**1. Daytime excess power mode:** In this mode, the output voltage of the PV array drives the boost converter based STATCOM for compensating the source as well as charges the battery (capacitor). Assume the inverter capacity,  $S$  is the rated peak power capacity of the PV array and with the active power  $P$  then the reactive power  $Q$ , capability is:

$$Q = \sqrt{S^2 - P^2} \quad (2.5)$$

According equation (2.5) after the PV- array generates the required active power the remained capacity is used for reactive power compensation.

**2.Day time mode:** When continuous compensation is required, if the PV output voltage is equal to the requirement of the boost converter input, the PV array can directly connect to the boost converter so as to step-up the voltage and match the dc link voltage of the three-leg VSC. In this mode, the battery is not charged.

**3. Nighttime mode (active power, P = 0):** In this mode, PV array output is idle and only the battery (capacitor) supplies the boost converter. In this condition, the whole capacity of the solar inverter can use for reactive power compensation. Thus, the reactive power supplied is equal to the rating power of the solar inverter (Q = S).

**2.4.2. PV- STATCOM Controller Modeling for Reactive Power Compensation:** Since the inverter based solar panels and the VSC based STATCOM devices are similar in structural operation and functionality as shown in Fig.2.6, these solar inverter have been used as STATCOM functionality with the addition of new control method termed as PV-STATCOM.

In this study, PV-STATCOM has been used as an automatic voltage regulator at PCC (main substation) of the selected wind farm. As shown in Fig.2.7, only the VDC\_ref of the conventional STATCOM have been replaced with MPPT controlled VDC\_ref voltage output of the solar array but, the control system and its' other components are not changed. In the PCC voltage regulation mode of operation of the PV-STATCOM, the PCC voltage is regulated through reactive power exchange between the PV inverter and the grid (PCC). In this system, the q-axis reference current, Iq\_ref controls the reactive power exchange between the PV-STATCOM and the grid (PCC). The measured signal, VPCC, at the PCC is compared with reference value VPCC\_ref and is passed through PI-2, to generate Iq\_ref. A phase-locked loop (PLL) in Fig.2.7 synchronizes the positive-sequence component of three-phase primary voltage VABC of the STATCOM converter with Vdq. The output of the PLL (angle  $\theta = \omega t$ ) is used to compute the d-axis and q-axis components of the AC three-phase voltage and current (labeled as Vdq or Idq on the diagram) using park's transformation.

The output of the AC voltage (V\_PCC), PI-2, is the reference current Iq-ref for the current regulator (Iq is current in quadrature with voltage which controls reactive power flow) by comparing it with q-axis measured current output. The output of the DC voltage, PI-1, is the reference current Id-ref for the current regulator (Id is current in phase with voltage

which controls active power flow) by comparing it with d-axis measured current output [7], [8], [9]. To maintain constant DC link voltage DC bus, is monitored and controlled through a controller PI-3 on direct axis current control loop which eventually defines the reference value Id\_ref for direct axis current control loop as shown in Fig.2. On the other hand, to regulate voltage at PCC through reactive power exchange, the PCC voltage is monitored and compared with PCC reference voltage, VPCC\_ref. The current signals are monitored from the PCC is then compared and passed through two PI controllers PI-3 and PI-4 to generate desired modulating signals md and mq respectively.

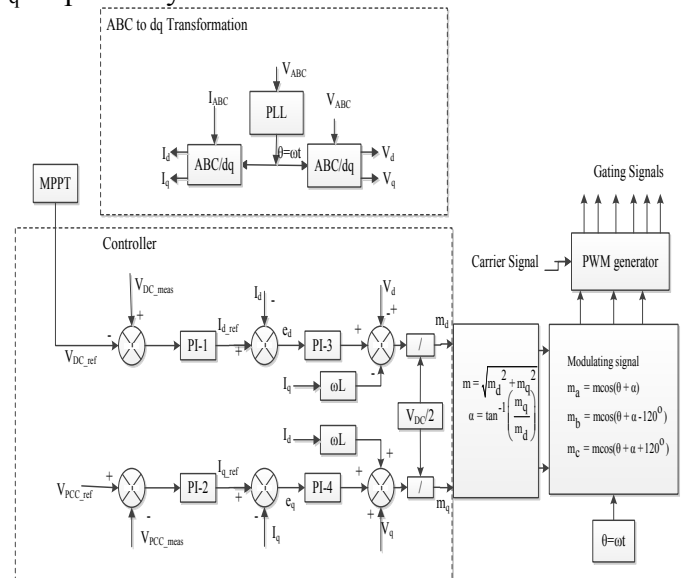


Fig.2.7. PCC voltage control schematic diagram of solar controller as PV-STATCOM

The real power, P and the reactive power, Q outputs in d-q co-ordinate system is given as [7]

$$\begin{cases} P = \frac{3}{2} [v_d i_d + v_q i_q] \\ Q = \frac{3}{2} [v_q i_d - v_d i_q] \end{cases} \quad (2.6)$$

To achieve the vector control scheme, the d-axis of the synchronous frame is aligned with the grid voltage vector, therefore the d-axis grid voltage is equal to its magnitude ( $v_d = v_g$ ), and the resultant q-axis voltage  $v_q$  is then equal to zero ( $v_q = 0$ ).

Then expressions the active and reactive power of equation (2.6) can be reduced to:

$$\begin{cases} P = \frac{3}{2} [v_d i_d] \\ Q = \frac{3}{2} [-v_d i_q] \end{cases} \quad (2.7)$$

From equations (2.6) and (2.7) the active and reactive powers are controlled by the d-axis and q-axis currents respectively.

The direct axis and quadrature axis voltages act as disturbance signals in these control loops and a decoupling factor of  $\omega L$  have been included to decouple the two control loops where,  $\omega$  is the angular frequency in rad/sec and  $L$  is the inductance at the output of the inverter

### 3. Results Analysis and Discussions

To overcome the above problem the study system was modeled as shown in Fig.3.1 with Matlab/PowerSim software. In this system the PV-STATCOM generates the required reactive power at the PCC of the WF and at the same time it can generate active power if there is no reactive power needed by the grid as indicated in the control system for the PV-STATCOM in Fig.2.5 above.

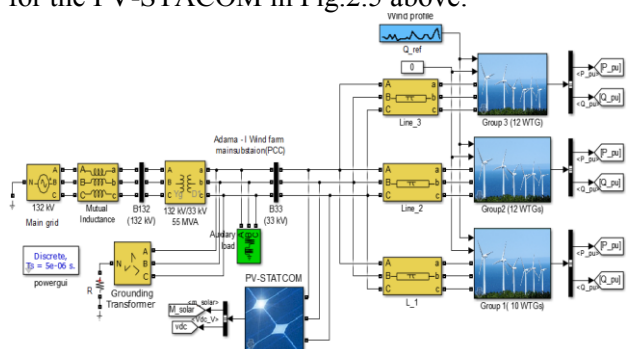


Fig.3.1, The overall system model in Matlab/PowerSim

#### 2.1.1. Simulation results of WTGs'

For the whole system of the selected wind farm WTGs' (34 in number) and its control systems, simulation based on the modeling as depicted in previous sections have been carried out using the dedicated MATLAB/PowerSim software as shown Fig.3.1 with disconnection of PV-STATCOM and the results are given Fig.3.2.

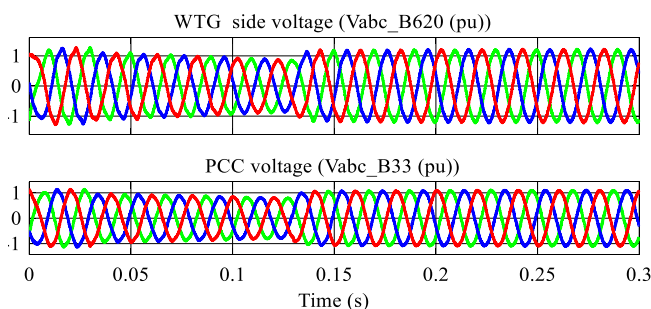


Fig.3.2, WTG side bus (B620V) and PCC bus (B33kV) output voltage waveforms

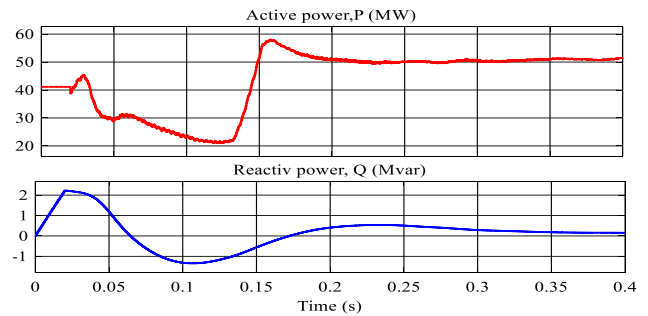


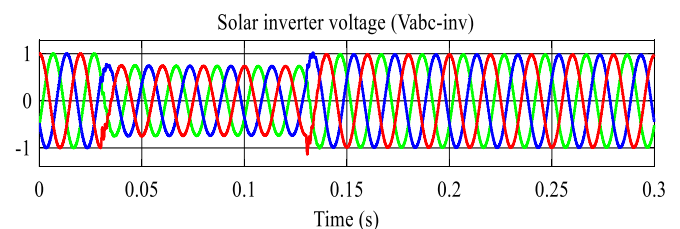
Fig.3.3, Active power (MW) and reactive power (MVar) outputs of the WTGs'.

The WTGs' side (B620) and PCC (B33) voltage (p.u) waveforms under normal operating conditions are determined as shown in Fig.3.2. These voltages have been considered as a base case study for the temporary over voltage study analysis. From Fig.5, the simulation have been done to generate an active power output of 51MW, which is Adama-I wind farm WTGs' total capacity and the reactive power to be nearly zero with a power factor consideration between 0.95 and 0.99 as shown in Fig.3.3.

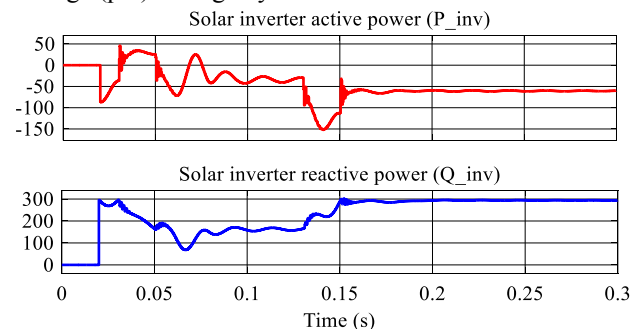
From Fig.3.3, the PMSG based WTG reactive power, Q(MVar) have positive and negative values, which indicates the generator is consuming and generating reactive power.

#### 2.1.2. Simulations results of PV-STATCOM

The PV-STATCOM output waveforms is done by disconnecting the PMSG wind turbine and its' 33kV connector transmission line of Fig.3.1. As we see from Fig.3.4 (b), the active power output magnitude of the PV-STATCOM is smaller as compared to the reactive power output. This indicates that the solar inverter is acting as conventional STATCOM.



(a) Grid connected PV-STATCOM three phase output voltage (p.u) during daytime



(b) Active (kW) and reactive power (kVar) outputs of PV-STATCOM without sunlight

Fig.3.4, Voltage, active and reactive power outputs



The per unit (p.u) values of the solar inverters three phase voltage wave forms is determined as shown in Fig.3.4 (a).

**3.1.3. Results to SLGF occurrence and effect of PV-STATCOM at the WTGs**

A Single Line to Ground (SLGF) occurrences at Adama-I PCC (B\_33kV bus) of the WTGs' is increasing the grid network voltages levels as shown in Fig.3.5 (a) specially and the wind turbine side voltages are also disturbed partially as shown in Fig.3.5 (b).

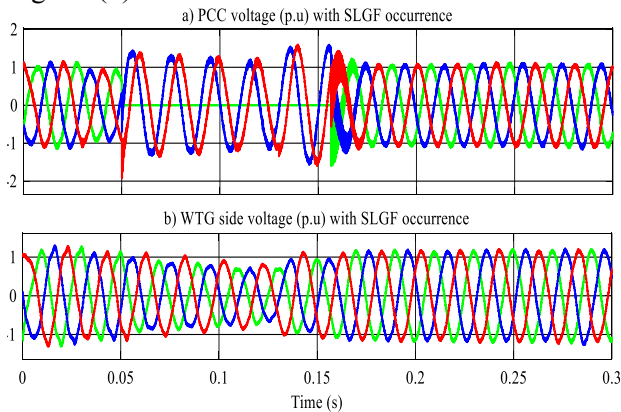


Fig.3.5, WTG side bus (B620V) and PCC bus (B33kV) output voltage waveforms with SLGF

From Fig.3.5 (a) when SLGF is occurred at the end of the transmission line near to the PCC of the WTGs' PCC single line phase voltage is forced to zero value for 0.1 second and this leads to overloading to the normally running phases. In addition, as shown in Fig.3.5 (b), this fault disturbs the WTGs' side voltage. If the WTGs' are unable to withstand to this voltage disturbance, they can be disconnect from main grid. However, this is uneconomical.

PV-STATCOM is considered at the wind farm main substation (PCC) to examine the effect of PV-STATCOM on the temporary over voltages in the study system for daytime and nighttime. In daytime analysis the remaining capacity of the VSC based solar inverter have been used for reactive power compensation after required active power generated. And for the case of night time since the solar panels are idle the whole capacity of the solar inverter have been used for reactive power compensation. Three phase voltages at PCC of WF with SLGF for 0% solar array power ( $P_{SA}=0$ ) and night is shown in Fig.3.6 (a). For sunny time hours the three phase voltages at PCC of WF is shown in Fig.3.6 (b).

As shown from the above Fig.3.6 (a and b) the magnitude of the PCC loaded phase voltage have been improved and limited within 1p.u value in magnitude with the installation of PV-STATCOM at the PCC of the WTGs'. However, without the use of

this device in the case of fault occurrence, the phase voltage magnitude violates the required limit 1p.u as shown in Fig.3.5 (a).

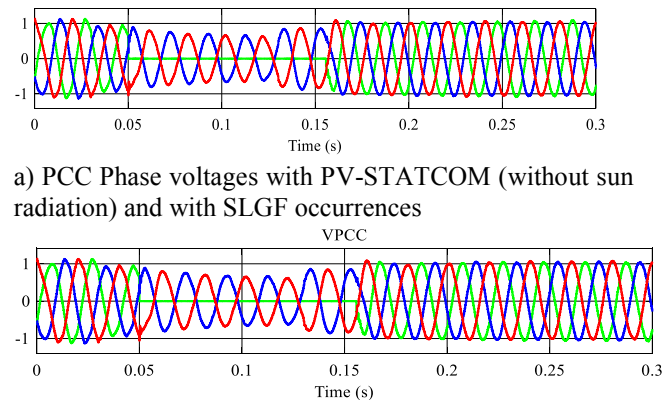


Fig.3.6, PCC voltage waveforms with the application of PV-STATCOM and SLGF

**3.2. System Model for Steady State Analysis**

The steady state network status namely bus voltage magnitude, active and reactive power flows, and transmission line ampacity (capacity) are evaluated using load flow studies in power world software with the use of 4-bus system as shown in Fig.3.7.

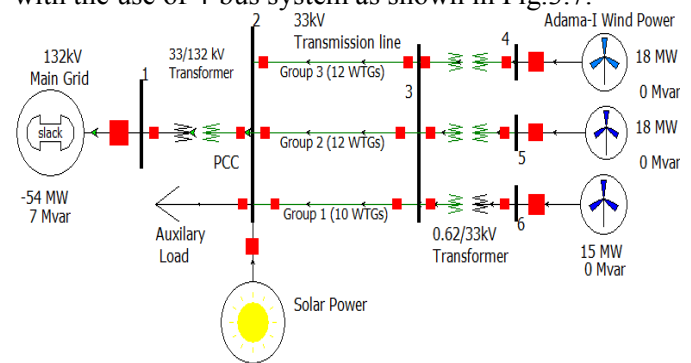


Fig.3.7. System model for steady state voltage analysis using power world software

The model in Fig.3.7 is analysed as a case study for two cases. The first case relates with the daytime in which the solar inverter generates 10MW active power. Second, in the nighttime case in which the solar inverter full capacity is used for reactive power compensation ( $Q=10MVar$  &  $P=0$ ). With the sending end main grid voltage set to 1.0 p.u, the steady state voltage results have been obtained without voltage regulation (reactive power compensation) for both the peak-load and off-peak load conditions. Peak loads ( $PLD = 6.48$  MW and reactive power,  $QLD = 21MVar$  have been used for daytime. off-peak loads of active power,  $PLD =$

3.38 MW and reactive power,  $Q_{LD} = 12.07$  MVar have been used for nighttime hours.

Load selection has been done to show the effect of more inductive load (e.g. Induction motors) demand at PCC of WTGs'. In addition, this inductive load is considered again to limit the steady state voltage rise at the PCC. Bus voltage magnitudes for daytime and nighttime loading conditions are given in Table 3.1. In this simulation the whole capacity (51MW) of Adama-I WTGs' have used to analyze the WF on grid steady state voltage variation. And the results of this analysis are given in the upcoming tables.

Table 3.1. Steady state voltage analysis at various nodes of the system for daytime and nighttime

Daytime(peak load) $P_{LD} = 6.48$ MW, $Q_{LD} = 21$ Mvar		Night time (off peak load) $P_{LD} = 3.38$ MW, $Q_{LD} = 12.07$ .Mvar	
Bus . No	Voltage (p.u)	Bu s. No	Voltage (p.u)
1	1.0000	1	1.0000
2	0.9407	2	0.9655
3	0.9408	3	0.9663
4	0.9423	4	0.9679

### 3.2.1 Effect of PV-STATCOM on Steady State Voltage Variations

By applying the PV-STATCOM to act as reactive power compensator the bus voltage limit ( $\pm 6\%$ ) of the rated required voltage of violations is seen in tables 3.2 & 3.3 is solved using this device as reactive Power compensator as given in table 3.4 & 3.5. As we observe from tables 3.4 & 3.5 with using PV-STATCOM we can regulate both the active and reactive/voltage power missing's in the wind farm networks.

Table 3.2, Case 1: 0% Solar array output,  $P_{SA} = 0.0$  MW,  $Q_{SA} = 0.0$  Mvar

$P_{WF}$	10	15	20	25	30	35	40	45	50	52
$V_{bus1}$	1.0000	1.0000	1.0000	1.0000	1.0000	1.0000	1.0000	1.0000	1.0000	1.0000
$V_{bus2}$	0.9570	0.9565	0.9552	0.9541	0.9521	0.9499	0.9474	0.9444	0.9409	<b>0.9395</b>
$V_{bus3}$	0.9586	0.9581	0.9571	0.9556	0.9535	0.9512	0.9485	0.9453	0.9417	0.9401
$V_{bus4}$	0.9607	0.9603	0.9592	0.9578	0.9554	0.9530	0.9502	0.9469	0.9431	0.9416
$I_{Line}$ (AMP)	198.22	283.99	371.72	461.23	551.95	643.87	736.85	830.97	926.36	964.15

Table 3.3, Case 3: 100% Solar array output,  $P_{SA} = 10$  MW,  $Q_{SA} = 0.0$  Mvar

$P_{WF}$	10	15	20	25	30	35	40	47	50
$V_{bus1}$	1.0000	1.0000	1.0000	1.0000	1.0000	1.0000	1.0000	1.00	1.00
$V_{bus2}$	0.9564	0.9555	0.9541	0.9523	0.9499	0.9473	0.9443	<b>0.9394</b>	<b>0.9369</b>
$V_{bus3}$	0.9579	0.9571	0.9557	0.9538	0.9512	0.9485	0.9454	0.9403	<b>0.9376</b>
$V_{bus4}$	0.9600	0.9592	0.9578	0.9559	0.9531	0.9504	0.9471	0.9419	<b>0.9391</b>
$I_{Line}$ (AMP)	198.54	284.24	372.22	462.05	553.18	645.61	739.20	872.33	930.32

Table 3.4, Steady state voltages with PV-STATCOM, case 1: 0% solar array output,  $P_{SA} = 0.0$  MW

$P_{WF}$	$V_{bus1}$	$V_{bus2}$	$V_{bus3}$	$V_{bus4}$	$I_{Line}$ (AMP)	$Q_{SA}$ (MVar)
10	1.0000	0.9570	0.9586	0.9607	198.22	
15	1.0000	0.9565	0.9581	0.9603	283.99	
20	1.0000	0.9552	0.9571	0.9592	371.72	
25	1.0000	0.9541	0.9556	0.9578	461.23	
30	1.0000	0.9521	0.9535	0.9554	551.95	
35	1.0000	0.9499	0.9512	0.9530	643.87	
40	1.0000	0.9474	0.9485	0.9502	736.85	
45	1.0000	0.9444	0.9453	0.9469	830.97	
50	1.0000	0.9409	0.9417	0.9431	926.36	0.00
52	1.0000	0.9424	0.9431	0.9445	961.80	1.0

Table 3.5, Steady state voltages with PV-STATCOM, case 1: 2% solar array output,  $P_{SA} = 10$  MW

$P_{WF}$	$V_{bus1}$	$V_{bus2}$	$V_{bus3}$	$V_{bus4}$	$I_{Line}$ (AMP)	$Q_{SA}$ (MVar)
10	1.0000	0.9564	0.9579	0.9600	198.54	
15	1.0000	0.9555	0.9571	0.9592	284.24	
20	1.0000	0.9541	0.9557	0.9578	372.22	
25	1.0000	0.9523	0.9538	0.9559	462.05	
30	1.0000	0.9499	0.9512	0.9531	553.18	
35	1.0000	0.9473	0.9485	0.9504	645.61	
40	1.0000	0.9443	0.9454	0.9471	739.20	0.00
47	1.0000	0.9408	0.9417	0.9432	870.98	0.5
50	1.00	0.9407	0.9415	0.9429	926.54	1.25

### 3.3 Economic benefit analysis of the PV-STATCOM

From the steady state analysis of tables 3.2 to 3.5, in the daytime at PV array power of 0% ( $P_{SA}=0$ ) the WTGs’ has been forced to generate power up to 50MW ( $50MW < 51MW$ ) and at PV array power of 100% ( $P_{SA}=10MW$ ) the WTGs’ have been forced to generate power up to 40MW ( $40MW < 51MW$ ) to meet the required voltage limit. These shows us in the case of low wind speed conditions the solar array can compensate the required power which have being generated by WTGs. With the use of 10MW PV array considered to act as STATCOM, we can save an additional cost to generate 5MW to 11MW wind power and, we can decrease the number of WTGs’ from 3 to 7 installation at the WF. Here using proper PV-STATCOM to keep node voltages to the required limit, we can connect 5MW and 11 MW an additional wind power during the daytime and nighttime respectively.

As deduced in this work PV-STATCOM have a dual advantage than conventional SVC/STATCOM which are limited in size and limited application i.e. is conventional SVC/ATATCOM are only used as reactive power/voltage regulators, but the PV-STATCOM are used both as reactive power regulators/voltage and as active power regulators.

### 4 Conclusion

Reactive power compensation and voltage support in wind farms have been successfully achieved with installation of PV-STATCOM at the wind farm main substation (PCC). From results, it has been observed that PV-STATCOM is able to improve the connectivity of the WTGs’ by regulating both the active and reactive power. For temporary over voltage analysis, SLGF have been considered near PCC of WF transmission line and simulation resulted the use of PV-STATCOM have been minimized the temporary voltage rise. Generally, PV-STATCOM has a dual advantage over STATCOM/SVC devices. The STATCOM/SVC are mostly limited to reactive power regulation or voltage regulation but the PV-STATCOM can regulate voltage, reactive power and active power of the WTGs’ network. Moreover, “STATCOM/SVC controller is more expensive than the PV-STATCOM controller.” Hence, we can generally increase WF generators connectivity and minimize the unnecessary costs on STATCOM/SVC by using the PV-STATCOM.

**References:**

- [1] Gonzalo Abad, Jesu'sLo'pez, Miguel A. Rodri'guez, Luis Marroyo and Grzegorz Iwansk, "Doubly Fed Induction Machine Modeling and Control for Wind Energy Generation" IEEE Inc, John Wiley & Sons, Inc., Hoboken, New Jersey, Canada, 2001
- [2] Thomas Ackermann, "Wind Power in Power Systems," John Wiley & Sons, Ltd, the Atrium, Southern Gate, Chichester, West Sussex PO19 8SQ, England, 2005
- [3] M. Muyeen, Ahmed Al-Durra and Hany M. Hasanien, "Modelling And Control Aspects Of Wind Power Systems," <http://dx.doi.org/10.5772/55090>, [online] March 20, 2013
- [4] Xiao-Ping Zhang, Christian Rehtanz and Bikash Pal, "Flexible AC Transmission Systems modeling and Control," ISBN: 3-540-30606-4, Springer, Berlin, 2012
- [5] N. G. Hingorani and L. Gyugyi, "Understanding FACTS; Concepts and Technology of Flexible AC Transmission Systems," IEEE ® Press book, 2000
- [6] Kalyan K. Sen and Mey Ling Sen, "Introduction to Facts Controllers Theory, Modeling, and Applications," ISBN 978-0-470-47875-2, John Wiley & Sons, Inc., Hoboken, New Jersey, Canada, 2009
- [7] BinWu, Yongqiang Lang, Navid Zargari and Samir Kouro, "Power Conversion and Control of Wind Energy Systems," IEEE-John Wiley & Sons, Inc. January 2011
- [8] Hydro China Corporation, "Master Plan Report of Wind and Solar Energy in the Federal Democratic Republic of Ethiopia (Final Version)," [unpublished], July 2001
- [9] "NASA's Surface Solar Energy: Data Set provides monthly average solar and wind radiation data, for everywhere on earth at," <http://eosweb.larc.nasa.gov/sse/>, [online], 2012